

Practical Design of Flight Control Systems: Some Problems and their Solutions

N.V. Kadam

Defence Research & Development Laboratory, Hyderabad-500 058

ABSTRACT

The flight control system design, though quite satisfactory on paper, many times gives surprises during the actual flight. This is due to unanticipated behaviour of the vehicle structure or the aerodynamic characteristics, or the higher-order dynamics and nonlinearities, etc. The paper describes few such cases in which problems were faced and their solutions found, and which gave satisfactory performance subsequently.

Keywords: Flight control system, flight vehicles, vehicle dynamics, control system design, flight tests, flight trials, time-slice approach

NOMENCLATURE

$C_{y\beta}, C_{y\delta}, C_p$	Aerodynamic parameters	T_E	Engine thrust
M_x	Maximum roll control torque	δ	Control deflection
d_z	Dead zone	L_R	Distance of engine CG from gimbal point
Q	Dynamic pressure	ζ	Damping ratio
f_y	Lateral acceleration	ω, ω_α	Natural frequencies
S	Laplace variable	M	Control torque
G_a, G_r, G_y	Transfer functions	$\phi, \dot{\phi}$	Roll angle, roll angle rate
s	Reference area		
K_a, K_R, K_S	Control gains		
r	Yaw angular rate		
L_a	Distance of gimbal point from the roll axis		

1. INTRODUCTION

The flight vehicles consist of aircraft, launch vehicles, and missiles. In the simplest of cases, these bodies have six degrees of freedom (6-DOFs) of motion in space. In addition, these have many high-frequency modes and nonlinearities, which make control system design complicated. The designer

makes many simplifying assumptions while designing the control system. The first such simplification is that the vehicle motion is decoupled. The pitch, yaw, and roll control system design is thus separately done assuming motion taking place only about one axis. The vehicle state and parameters also change continuously due to burning of fuel, change in velocity, and trajectory parameters such as altitude, dynamic pressure, etc. The design of this time-varying system is carried out using time-slice approach, where the vehicle and the trajectory parameters are assumed to remain constant for a short period of time. The vehicle transfer function is then obtained using small-angle perturbations. The study is repeated at a regular interval of time till the entire flight zone is covered. The design is then mechanised to give a gain schedule for the entire flight duration. Subsequently, higher-order dynamics are incorporated and the stability margins are checked for adequacy. The validation of the design incorporating all nonlinearities is carried out using 6-DOFs trajectory simulation.

This design methodology gives quite satisfactory results during flight testing. During actual implementation of the control logic in onboard computer, the designer has to address many other issues to get satisfactory performance of the system. This does not involve actual working out the gains or design of compensators, however, the performance of the control system will be affected, or sometimes, the design may become totally ineffective if those issues are not properly addressed. Resolution of signals in proper axes frames, sensor characteristics, actuator characteristics, mountings of sensors or actuators, limiting the operational zones and various signals, are some of these factors.

A designer needs to incorporate robustness features wherever possible to make the system robust in unforeseen circumstances. Many times, the awareness about the need of such features comes only after encountering catastrophic failures during the flight trials. These robustness features when seen individually, appear minor in nature and never get adequately publicised. Their significance, many times, is not appreciated by the new designers, who mainly concentrate on the gain schedule and compensator

design. Sometimes, it is observed that published literature also indicates such provisions. However, its importance is not realised and is quickly forgotten till there is another mishap.

This paper intends to discuss few such issues with a background information to highlight the importance of the provision.

2. CONTROL GAIN ADAPTION

As discussed above, the vehicle dynamics continuously changes during flight due to changing mass, moment of inertia, centre of gravity, and the trajectory parameters such as dynamic pressure, Mach number, etc. Time-slice approach is used as a standard practice in which the vehicle parameters are assumed to remain constant for a short period of time¹. The control gains are designed to give the required performance. The design is carried out at regular interval of time during a flight trajectory and the gains schedule is thus arrived. The gain adaptation is then done differently by different designers considering the type of vehicle for which the design is carried out.

For launch vehicles, the trajectory is very well-defined long before the actual flight. The gains are generally made a function of time. It is subsequently tested for adequacy for expected variations in thrust, centre of gravity, and aerodynamic perturbations, giving maximum possible rearward or forward variations of centre of pressure.

For missiles, the trajectory is not so well-defined in advance and the designers have made the gains a function of missile velocity or the dynamic pressure. The design needs to be validated for the entire flight zone and perturbations in inertial parameters, propulsion, and aerodynamic data.

For aircraft, one needs to cater for takeoff, landing, and the remaining flight regime, depending on whether it is a transport aircraft or a fighter. It is observed that gains are stored as huge, two-dimensional tables with altitude and Mach numbers as dimensions. Extensive validation studies are then carried out to check for the satisfactory performance at various grid points and interpolation points.

The above methods of gain adaptations have the following disadvantages:

The same velocity may be obtained during the powered phase and the descent phase. The missile inertial parameters could be quite different, and hence, gains as a function of velocity may not give satisfactory performance. Similarly, same dynamic pressure could occur at quite different values of inertial parameters or Mach number. Hence, the same gains obtained as a function of dynamic pressure could give unsatisfactory performance in different trajectory phases.

The gains used as a huge table in two dimensions is likely to involve a tedious and time-consuming design cycle if the vehicle characteristics are updated, which generally happens in a development project.

A completely adaptive design scheme has been used to overcome the above disadvantages. The method has been extensively tested by simulating a large number of trajectories and also a number of flight trials, and it has been found to give satisfactory performance, both in simulation and flight trials.

The scheme consists of the following features:

- Determination of vehicle transfer function
- An algorithm for computing gains
- Specification of dominant poles or control bandwidth.

Figure 1 shows a latax (lateral acceleration) control block diagram for yaw plane. The vehicle dynamics² for perturbed motion is given by

$$f_y = \dot{v} + ur = y_v v + y_r r + y_\delta \delta$$

$$\dot{r} = n_v v + n_r r + n_\delta \delta$$

The closed-loop transfer function is given by

$$\frac{f_y}{f_{yd}} = \frac{K_s G_{\ddot{y}}}{1 + K_s K_R G_a G_r + K_s K_a G_a (G_{\ddot{y}} + C_s G_r)}$$

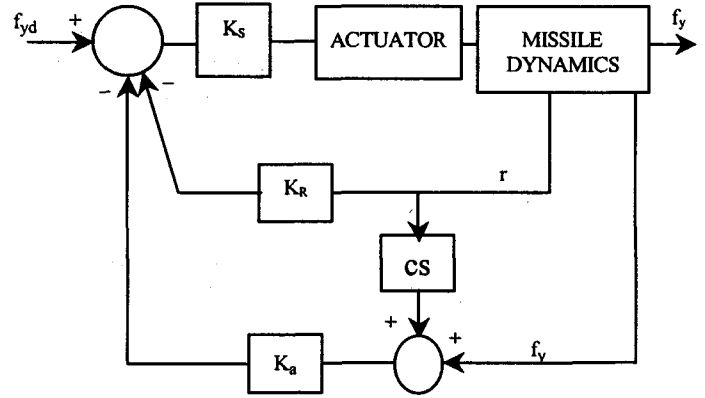


Figure 1. Yaw plane-latax control system

where

$$y_v = -C_{y\beta} QS / (MV)$$

$$y_\delta = C_{y\delta} QS / M$$

$$n_v = C_{y\beta} QS (C_p - C_g) \frac{d}{I_y V}$$

$$n_\delta = -C_{y\delta} QS \frac{dl_c}{I_y}$$

$$y_r \approx n_r \approx 0$$

$$G_a = \frac{\omega_a^2}{s^2 + 2\zeta_a \omega_a s + \omega_a^2}$$

$$G_r = \frac{r(s)}{\delta(s)} = \frac{n_\delta s - n_\delta y_v + n_v y_\delta}{s^2 - (y_v + y_r)s + y_v n_r + n_v v - n_v y_r}$$

$$G_{\ddot{y}} = \frac{y_\delta^2 s - y_\delta n_r s - u(n_\delta y_v - n_v y_\delta)}{s^2 - (y_v + y_r)s + y_v n_r + n_v v - n_v y_r}$$

The fourth-order characteristic equation is now equated to

$$(s^2 + 2\zeta_a \omega_a s + \omega_a^2)(s^2 + 2\zeta \omega s + \omega^2)$$

where the ζ_d and ω_d indicate the desired pole locations, and ζ and ω indicate the unspecified poles. The solution for control gains can be obtained using the following steps:

Step 1. Specify ζ_d and ω_d

Step 2. Solve for $K_s K_R$ and $K_s K_a$ products by equating coefficient of like powers of s on both the sides.

Step 3. Obtain the value of K_s using the products obtained in *Step 2* and equating steady state closed-loop gain to unity.

Step 4. Individual gains K_s , K_R , and K_a can then be obtained.

The usability of the solution now depends only on the choice of ω_d (ζ_d is generally chosen as 0.6 to 0.7).

Since the control torque is now only dependent on dynamic pressure, ω_d is made a function of dynamic pressure. This is essential since one cannot expect the same bandwidth of control system at high and low-dynamic pressures. If one puts the same specifications in low-dynamic pressure region, the algorithm will give the values of gains. However, those will be very high gains and the control surfaces will quickly saturate. Further, the δ required will also be very high. The system will not be able to give the required speed of response due to saturation. Hence, it is essential that the desired bandwidth be made a suitable function of dynamic pressure. Figure 2 gives a sketch of the rule adopted for the desired ω_d as a function of dynamic pressure.

To make the control fully adaptive, it only needs to determine the vehicle transfer function. This is achieved in the following manner:

- (a) Mass, centre of gravity, and I_{yy} were made as a function of time (due to propellant burning). One may use it as a table look up or a polynomial on time.
- (b) $C_{y\beta}$, C_p , $C_{N\delta}$ were obtained as a function of the Mach number and may be a table look up or

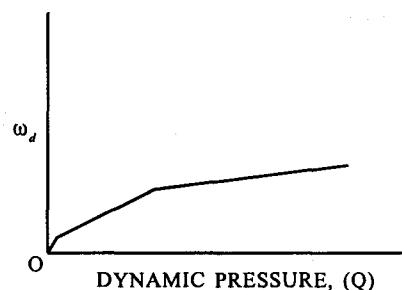


Figure 2. Desired ω_d as a function of dynamic pressure

polynomial. In the design under discussion, the parameters for a fixed value of α were obtained as a cubic polynomial of the Mach number. Three different Mach number zones were considered for the polynomial fitting.

- (c) The dynamic pressure and Mach number were obtained by obtaining air density and sound velocity as the polynomials in altitude from standard atmosphere and instantaneous missile velocity.

The design also incorporated additional compensator for achieving the desired gain and phase margins, and filters to handle structural flexibility. The design was tested extensively by simulation for a large number of trajectories and a number of flight tests and it was found to be adequately robust.

It is known that the aerodynamic parameters, $C_{y\beta}$ and C_p are also a function of the angle of attack. If an aircraft or a missile is operating at high angle of attack for a significant duration of time, one may also re-evaluate $C_{y\beta}$ and C_p around operating values of α to make the design more robust.

3. ROLL OSCILLATION DUE TO TAIL-WAG-DOG EFFECT

The particular case relates to a missile having liquid propellant and two-engine configuration. The two engines were mounted in pitch plane and could be moved in pitch and yaw planes. Both the engines were moved simultaneously for pitch and yaw control and differentially for achieving roll control. The simplified dynamic equation for roll motion is as follows:

$$I_x \ddot{\phi} = 2T_E L_a \delta + 2M_R L_R L_a \ddot{\delta}$$

The initial design had stability margins of

Gain margin = 8.6 dB

Phase margin = 37°

Peak after TWD frequency = -8.5

The flight performance showed 14 Hz oscillations in the roll channel which could not be reproduced in simulation. The simulation used δ and $\ddot{\delta}$ as obtained from the second-order actuator transfer function. The recovered flight hardware showed damage at the base of engine lug to which the actuator was connected.

Obviously, high stresses were induced due to roll oscillations. Further, it was felt that the $\ddot{\delta}$, as obtained from the second-order dynamic equation, may not be indicative of the actual $\ddot{\delta}$ experienced by the engine due to lug-base joint flexibility. Hence, the actual acceleration experienced was derived by measuring the acceleration at the exit plane and dividing it by the gimballed engine length, L (Fig. 3).

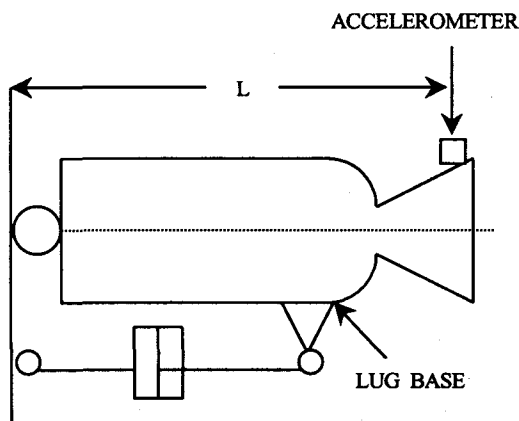


Figure 3. Gimbaled engine configuration

When this derived $\ddot{\delta}$ was introduced, the hardware-in-loop simulation reproduced the roll oscillations as experienced in the flight.

Figure 4 shows an illustrative gain plot for the roll control system. The gain plot shows a hump after the notch. The notch corresponds to the tail-wag-dog frequency. For this input frequency, the

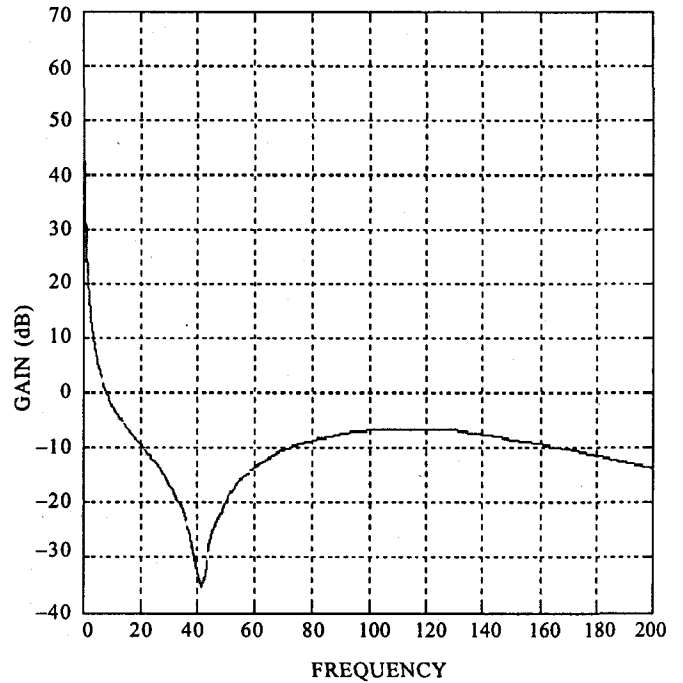


Figure 4. Gain plot for roll control system

control torque is completely cancelled by the engine inertia torque. For frequencies higher than this frequency, the inertial torque due to engine inertia will dominate the control torque and net torque will have opposite polarity to that of the required control torque polarity.

To avoid oscillations due to tail-wag-dog effect, the gain plot needs to be sufficiently attenuated after the notch. The oscillation problem was solved using a second-order filter in the control loop which gave a gain peak of -25.5 dB after tail-wag-dog frequency. With this filter, the flight performance showed a very smooth roll control.

4. FLEXIBLE MODE INSTABILITY DUE TO CONTROL-STRUCTURE INTERACTION

The design of flight control system is carried out in following steps:

- Step 1. Control system gain schedule design assuming vehicle as a rigid body
- Step 2. Checking the stability margins after incorporating structural flexibility. Design suitable filters to ensure stability of structural modes.

Step 3. Perturb the vehicle data within the expected bounds and check for instability.

The design procedure is found to be quite satisfactory in a number of flights.

The control-structure interaction generally enters the control loop through sensor and actuator mountings. As a general guideline, the rate gyros and angle sensors are placed near the antinode of the first mode and the accelerometers are put at the nodes so that the sensor senses a minimum signal due to flexible modes. Many times, these locations are practically not possible due to nonavailability of space. In such a case, the detailed analysis is carried out incorporating the structural mode dynamics and adequate stability margins are provided. As a general rule, the stability studies are also carried out by perturbing the mode shape data within the expected bounds.

In spite of all the above studies, one of the missile flight showed unstable bending mode, leading to diverging oscillations and structural failure (Fig. 5).

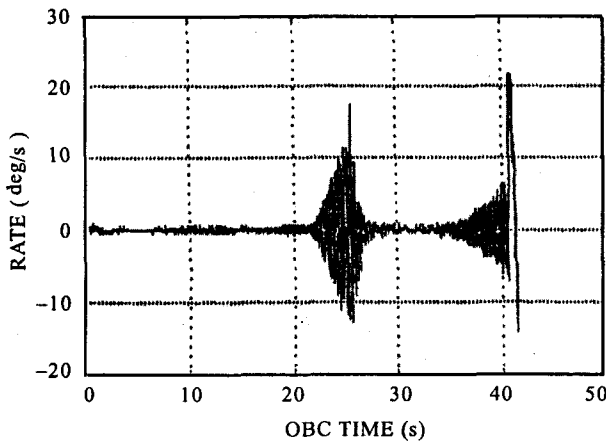


Figure 5. Unstable bending mode oscillations

For the case under study, two sensor packages were used (Fig. 6). One sensor package was put near the antinode to be used for the control system during the first stage of flight. The other sensor package was placed inside the equipment bay nearer to the nose and was to be used after the first stage was separated. The sensed angular rate by the rate gyros will be as follows:

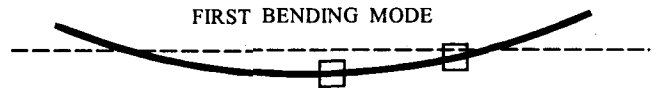
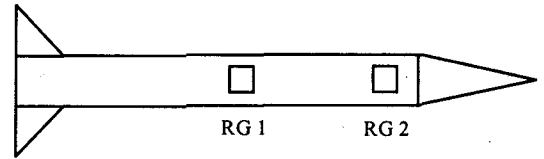


Figure 6. Vehicle sketch showing rate gyros along X-axis

$$Q_1 = Q_R + \frac{d\phi_1(l)}{dl} \dot{q}_1(t)$$

$$Q_2 = Q_R + \frac{d\phi_2(l)}{dl} \dot{q}_2(t)$$

where Q_R is the rigid body rate.

Assuming dominant contribution only from the first mode, the amplitude of the rates sensed by the two rate gyros will be in the ratio of mode slopes (ie, $\frac{d\phi_1(l_1)}{dl} / \frac{d\phi_1(l_2)}{dl}$) at the two sensor locations. For the preflight-predicted mode shape data, this ratio was expected to be around 1/8. The flight data showed that the amplitude ratio is about - 4/8, indicating that the rate gyro placed near the antinode was not only reading higher slope but the slope had an opposite sign to the expected one.

The ground resonance test was carried out to verify this result. The test showed that the sensor was in fact sensing as per flight due to local deformation in the mode shape. This highlights the importance of fully instrumented ground resonance test (GRT).

The ground resonance test also showed another anomaly. The rate gyro package, consisting of two rate gyros (R_p and R_y) for pitch and yaw control system, was mounted as shown in Fig. 7(a).

The repeated test results showed that the rate gyro with sensitive axis mounted along the radius showed the correct polarity but the rate gyro whose sensitive axis was mounted parallel to the tangent

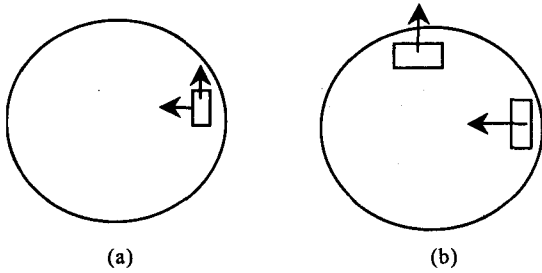


Figure 7. Rate gyro package: (a) initial rate gyro mounting and (b) revised rate gyro mounting.

was sensing a phase reversal. The problem was solved by putting two separate rate gyros 90° apart with both having their sensitive axis along the radius as shown in Fig. 7(b).

5. ROLL OSCILLATIONS AT HIGH ANGLE OF ATTACK

A roll control system design is relatively simple. The missile under consideration is a subsonic missile having imaging infrared seeker. It was observed that when the missile was executing a high lateral acceleration (latax) manoeuvre, it was experiencing roll oscillations with high roll rate (Fig. 8).

The high roll rates were not acceptable for the imaging infrared seeker. These roll oscillations could not be reproduced in trajectory simulation. Working backwards, the required disturbance torque to produce the observed motion was computed. It

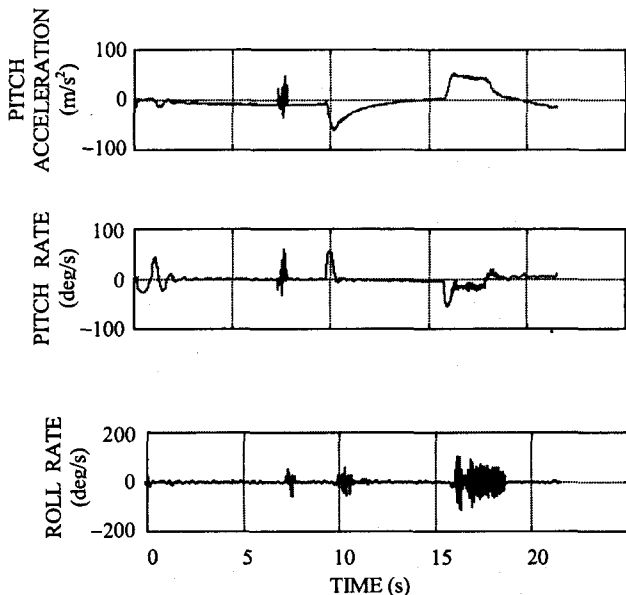


Figure 8. Roll oscillations at latax manoeuvre

was observed that the disturbance torque is changing directions. To understand this characteristic, the wind tunnel testing was carried out and the test was repeated a number of times for each setting.

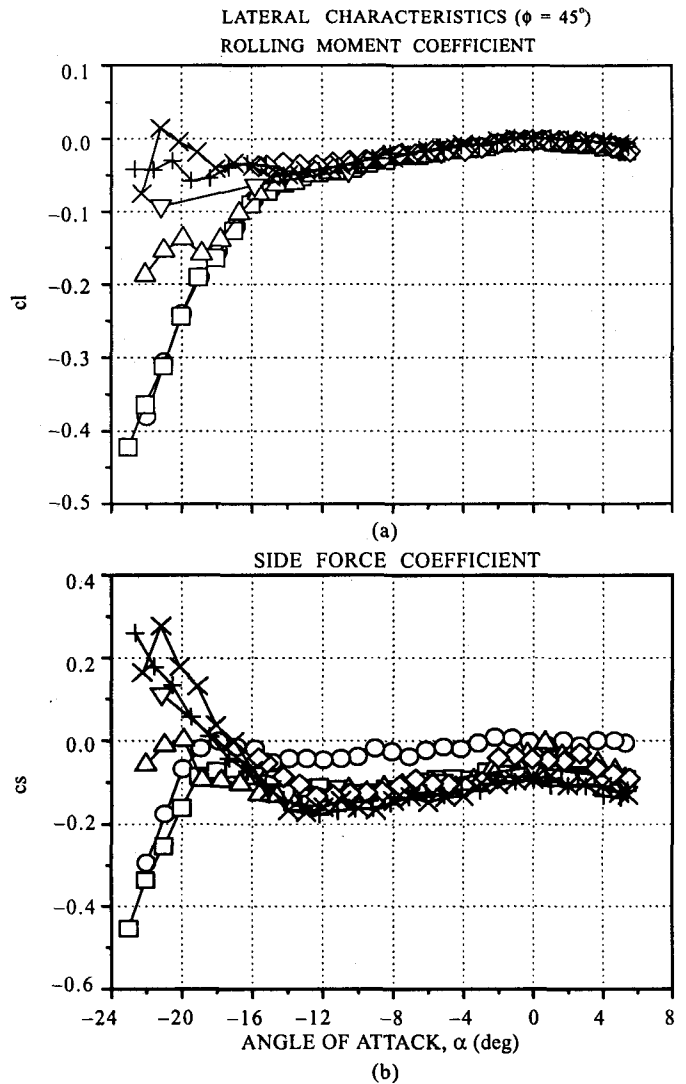


Figure 9. Repeatability of test data: (a) rolling moment coefficient and (b) side force coefficient before providing a band.

The test results are shown in Fig. 9, which shows that though the repeatability of the normal force and pitching moment coefficient was very good, the repeatability for side force and the rolling moment coefficient was satisfactory only up to an angle of attack, $\alpha = -16^\circ$ and beyond that, the values were very different for the same setting, and sometimes, even changing the sign. It was thought that non-repeatable data was due to vortices

being set at high angle of attack, giving unpredictable performance. Aerodynamic scientists provided a ring on the missile (Fig. 10) to fix the vortex separation.

The wind tunnel tests were repeated and the results are shown in Fig. 10, which show that the results are quite repeatable. Flight tests with ring fitted on the missile are yet to be carried out.

6. FLEXIBLE STRUCTURE AERODYNAMICS

Large length-to-diameter (L/D) ratio missiles, while executing manoeuvres undergo structural bending due to aerodynamic load distribution and vehicle's inertial parameters. The flexed shape depends on the EI distribution along the length and gives rise to changes in local angle of attack, and thus brings change in aerodynamic load. This gives rise to mismatch in performance of the control system during flight and simulation. The effect of vehicle flexing on aerodynamic parameters was subsequently estimated and indicated by the ζ factor where

$$\zeta_{C_{N\alpha}} = \frac{C_{N\alpha flex}}{C_{N\alpha rigid}}$$

$$\zeta_{C_{N\delta}} = \frac{C_{N\delta flex}}{C_{N\delta rigid}}$$

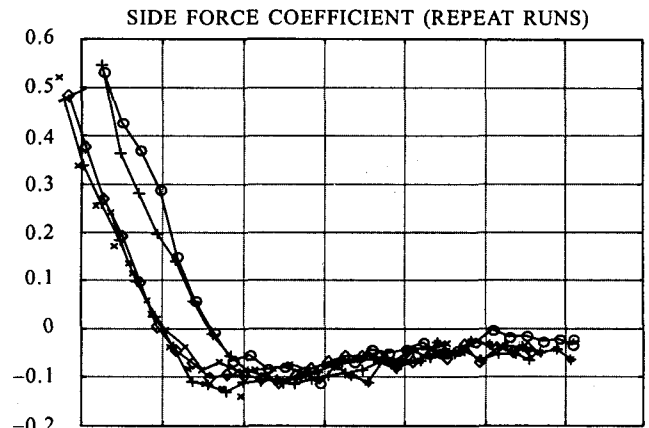
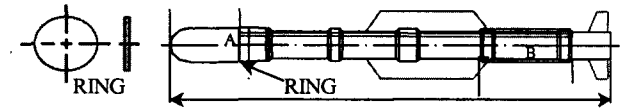
The missile under consideration had two control surfaces: (i) wings for lateral acceleration control and (ii) tail control panels (TCPs) used for providing damping torque for lateral acceleration control system and also control torque for roll.

The aerodynamic loads acting on tail control panels created offset loading on the main fin resulting in its twisting, leading to a significant reduction in net control torque due to TCP deflections.

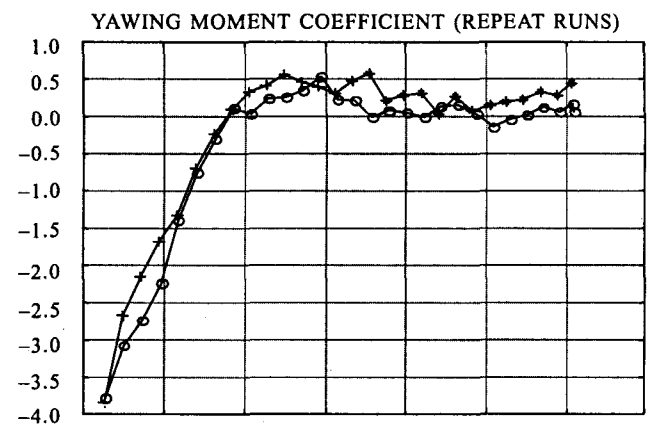
The detailed evaluation of ζ factors showed that

$$\zeta_{C_{N\delta}} = 0.933$$

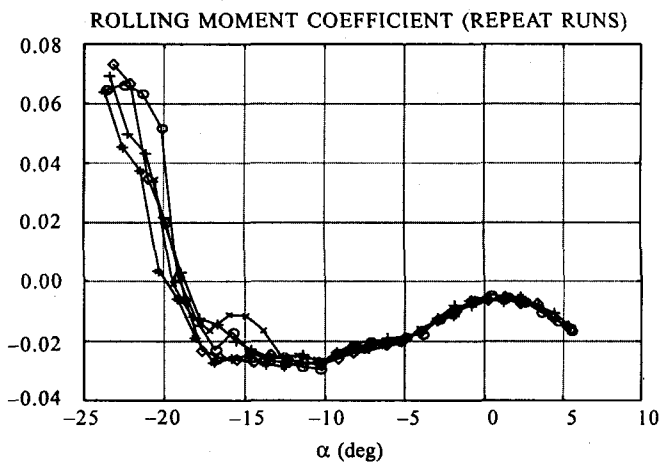
$$\zeta_{C_{N\delta wing}} = 1.136$$



(a)



(b)



(c)

Figure 10. Repeatability of: (a) side force coefficient, (b) yawing moment coefficient, and (c) rolling moment coefficient after providing a band.

$$\zeta_{C_{N\delta TCP}} = 0.671$$

$$\Delta_{C_P} = -0.0976$$

$$\zeta_{C_{M\delta TCP}} = 0.686$$

This indicates that there is a significant reduction in control effectiveness of TCP and the control gains need to be designed considering this ζ factor.

7. SPIN-TOLERANT LOGIC FOR A REACTION CONTROL SYSTEM

Reaction control systems are generally used for stages operating outside the sensible atmosphere. Considering a roll control system, the usual control logic is as follows:

$$e = \phi + K_R \dot{\phi} \text{ assuming } \phi_c = 0$$

$$\begin{aligned} \text{then } M &= -M_x && \text{if } e > d_z \\ &= M_x && \text{if } e < -d_z \\ &= 0 && \text{if } |e| < d_z \end{aligned}$$

The block diagram of the roll control system is shown in Fig. 11.

The necessity of using spin-tolerant control logic for this system is discussed for the following design parameters:

$$K_R = 0.5$$

$$d_z = 1^\circ$$

Rate gyro saturation limit = 30°/s

Angular sensor range = ± 180°

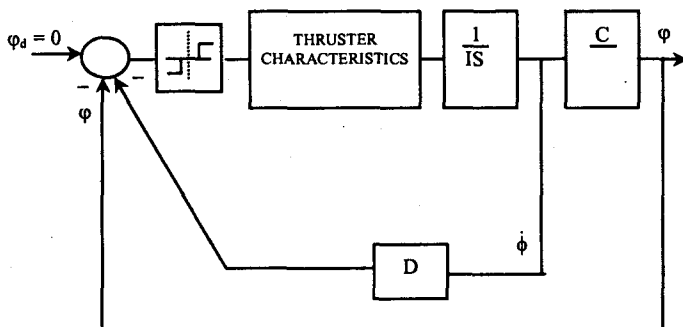


Figure 11. Block diagram of roll control systems.

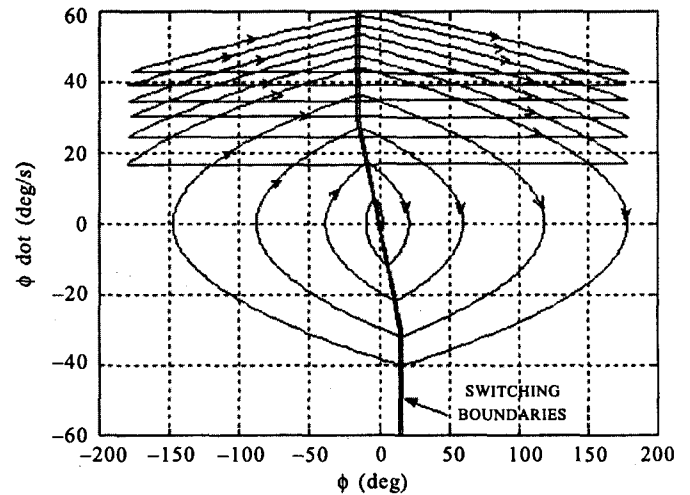


Figure 12. Systems response without spin-tolerant control logic

For the vehicle under consideration, the above control system was used for a second-stage roll control system. The first stage was using aerodynamic control and electro hydraulic actuation system. After the stage burn out, one of the actuator developed a problem, leading to maximum deflection of the control surface. The vehicle developed a spin rate and rate gyro was saturated. After the stage separation, the reaction control system came into operation, however the performance was not satisfactory due to the following reasons:

- (a) Rate gyro saturation results in change of switching boundaries (Fig 12).
- (b) The sign of angle changes as soon as the angle passes through ±180°. This results in change of sign of the error function and leads to firing of wrong reaction control system motor. Thus, the reaction control system will give torque to increase the spin rate instead of reducing it.

$$\begin{aligned} e &= \phi + K_R \dot{\phi}_{sat} \\ &= \phi + 15^\circ \end{aligned}$$

(using $K_R = 0.5$, $\dot{\phi}_{sat} = 30^\circ/\text{s}$).

For a dead zone, $d_z = 1^\circ$

$$e > 1^\circ \text{ for } -14^\circ < \phi < +180^\circ$$

$$< -1^\circ \text{ for } -180^\circ < \phi < -16^\circ$$

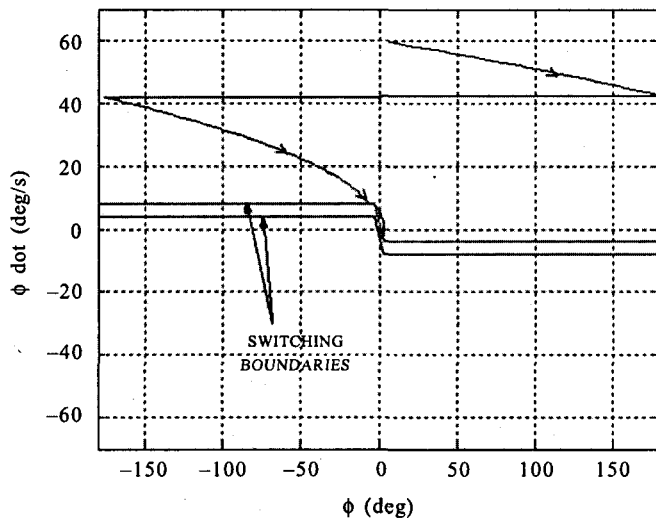


Figure 13. Systems response with spin-tolerant control logic

Thus in a total 360° , reaction control system will attempt to reduce the spin rate over 194° but act to increase the rate over 164° and dead zone of 2° . Figure 12 shows the sketch of the missile state in phase plane for an initial condition $\phi = 0$, $\dot{\phi} = 60^\circ/\text{s}$. It will take a long time to kill the spin rate and come to normal operation scenario.

This scenario can be corrected by providing a simple spin-tolerant logic as follows:

$$\text{If } |\phi| > \phi_{sat}$$

$$\phi_s = \phi_{sat} \text{SGN}(\phi)$$

Then this ϕ_s is used in the error function calculation. The phase plane sketch of switching boundary will appear as in Fig. 13 for $\phi_{sat} = 3^\circ$ and the missile state will appear as shown. It may be seen that the reaction control system is now attempting to bring down the spin rate at all times. As soon as the state enters within the switching boundaries, the reaction control system stops and the missile state is brought down on its own without using fuel. The value of ϕ_{sat} can be set slightly above the dead zone value to have a satisfactory operation of the whole system.

It may be seen that the logic appears very simple and its significance may not be understood by the newer designers. However, it has great significance from the point of view of making the

system very robust and tolerant to system failures. The mission may lead to a complete success even if some short duration failures occur. This logic is also useful for quick settling down of the system state after stage separation disturbances to normal operating zone.

8. SOFTWARE PROTECTIONS TO AVOID ABNORMAL FUNCTIONING OF FLIGHT CONTROL SYSTEM

In Section 7, it is demonstrated how a control system can get into difficulty due to change in sign of Euler angles when it passes through $\pm 180^\circ$. It is also demonstrated how the problem can be handled by limiting the angle variable to be used in error function even though the sensor is sensing the large angles. Many times, flight software uses quaternions instead of Euler angles. Due to relatively less frequent use of quaternions compared to Euler angles, the protective features in respect of quaternions are not familiar to the scientific community. It can be easily proved that the comparative protective features for quaternions and Euler angles are as given below:

(a) Limiting the angular range between 0° to $\pm 180^\circ$

$$\text{If } \theta > +180^\circ, \theta = \theta - 360^\circ$$

$$\text{If } \theta < -180^\circ, \theta = \theta + 360^\circ$$

This is equivalent to:

Limiting q_0 to $q_0 \geq 0$, where the quaternion is given by $Q = [q_0, q_1, q_2, q_3]$ and q_0 is a scalar part of the quaternion. To ensure this condition, the software protection is given by

If $q_0 < 0$, multiply all the four components of quaternions by (-1)

(b) Protection of angular errors to the range 0 to $\pm 180^\circ$.

Inspite of limiting all the angles to a range of 0 to $\pm 180^\circ$, the angular errors can violate this range in specific cases. For example, let the desired $\theta_d = 175^\circ$ and the actual vehicle angle is $\theta = -175^\circ$. The vehicle needs to be rotated through 10° only to align with the desired orientation. However, the computed error will be

$$\theta_d - \theta = 175 - (-175) = 350^\circ$$

The control system, if not given appropriate protection, will attempt to align the vehicle with the desired orientation by rotating through 350° and will develop large angular rates in the process, leading to failure.

Hence, it is essential to provide protection to angular errors as well, even though the angles themselves are already given the protection. In case of quaternions, the same thing is achieved by providing protection to error quaternion q_e as follows:

$$q_e = Q_M^{-1} Q_D$$

where Q_M is the actual quaternion and Q_D is the desired quaternion.

If $q_{e0} < 0$, multiply all the components of q_e by (-1).

9. CONCLUSION

The paper describes some experiences with practical design of the flight control systems. It highlights the importance of learning from experience and indicates that only the analytical designs of gain schedule and compensators/filters is not adequate to give trouble-free flight control system. There

are many such small ideas which have great significance in making the flight control system very robust and trouble-free.

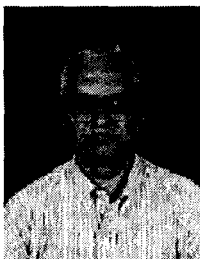
ACKNOWLEDGEMENT

The author is the investigator in some of the problems discussed above. There were many other investigators involved in post-flight analysis and testing of the systems, thus, making difficult to mention their names. Though the author has not investigated the roll oscillations at high angle of attack and flexible structure aerodynamics, the topics are discussed here only to highlight the importance of learning from flight trial data. The author thanks Dr Paneerselvam, Director, Aerodynamics and Shri Patrick D'Silva, Scientist, Flight Structures, for supplying the necessary data used for illustrating the point on rolling moment coefficient and ζ - factor for flexible structure, respectively.

REFERENCES

1. Greensite, A.L. Analysis and design of space vehicle flight control systems. Spartan Books, 1970.
2. Garnell, P. Guided weapon control systems. Permagon Press, 1980.

Contributor



Mr N.V. Kadam obtained his MTech (Electronic Engg) from the Indian Institute of Technology Bombay, Mumbai. He is a designer of control systems for India's first satellite launch vehicle SLV-3 and a digital autopilot for *Prithvi* missile. He also contributed to the autopilot design of ASLV and PSLV launch vehicles and almost all-missile programmes of India. He developed generalised software for control-structure interaction studies, including propellant slosh and gimballed engine inertia. He has been Director, Systems and Associate Director of Defence Research & Development Laboratory, Hyderabad. Presently, he is Emeritus Scientist and Director, Weapon Systems. He received *DRDO Technology Award* (1995) as a team leader and *DRDO Award for Performance Excellence* (1998). His current interests are: Analysis, design and simulation of flight control systems, trajectory shaping, and mission analysis studies. He is a life member of Astronautical Society of India, Aeronautical Society of India, and Systems Society of India. He was elected as Fellow of Indian National Academy of Engineering (1996) and has been a member of the Sectional Committee for two terms. He was also elected Vice-president of the Systems Society of India for two terms.